Solid state organic X-ray detectors based on Rubrene single crystals

Journal:	*IEEE Transactions on Nuclear Science*
Manuscript ID:	TNS-00087-2015.R1
Manuscript Type:	RTSD
Date Submitted by the Author:	n/a
Complete List of Authors:	Basiricò, Laura; University of Bologna, Department of Physics and Astronomy Ciavatti, Andrea; University of Bologna, Department of Physics and Astronomy Sibilia, Mirta; University of Trieste, Department of Engineering and Architecture Fraleoni-Morgera, Alessandro; University of Trieste, Department of Engineering and Architecture; Elettra Sincrotrone Trieste S.C.p.A, ; CNR-NANO S3, Trabattoni, Silvia; University of Milano Bicocca, Department of Materials Science Sassella, Adele; University of Milano Bicocca, Department of Materials Science Fraboni, Beatrice; University of Bologna, Department of Physics and Astronomy
Standard Key Words:	X-ray detectors, Radiation detectors

Solid state organic X-ray detectors based on Rubrene single crystals

Laura Basiricò, Andrea Ciavatti, Mirta Sibilia, Alessandro Fraleoni-Morgera, Silvia Trabattoni, Adele Sassella and Beatrice Fraboni

***Abstract*— In this work we report the results on the first investigation on Rubrene single crystals as solid state direct ionizing radiation detectors. With the aim to understand how electrical properties, and in particular a large charge carrier mobility, affect the radiation detection process in organic semiconducting single crystals, we compare the detection performance of Rubrene-based devices with those of 1,5-dinitronaphthalene (DNN)-based ones. DNN has been recently proven to be a stable and reliable X-ray direct detector, operating at very low voltages, in air and at room temperature, with a carrier mobility values about two orders of magnitude lower than Rubrene. We demonstrate here that the large charge carrier mobility of Rubrene crystals does not result in a better X-rays detection performance. In fact, Rubrene devices are here shown to be less performing as detectors, with lower sensitivity to X-rays, poorer stability, reproducibility and longer rise and decay times of the signal than DNN-based devices.**

***Index Terms*— Direct X-ray detectors, Sensors, Rubrene, 1,5-dinitronaphthalene, Organic Single Crystals**

I. Introduction

VERY recently we demonstrated [1][2] how Organic Semiconducting Single Crystals (OSSCs) grown from solution can be used as room temperature, low-voltage direct X-ray detectors. The direct detection approach, i.e. a direct conversion of ionizing radiation into an electrical signal, results in an improved signal-to-noise ratio with the advantage of a real-time radiation detection if compared to the indirect approach, in which organic materials have been proposed both as scintillators [3] and as photodetectors to be coupled to a scintillating material [4][5]. The studies on the application of organic materials in ionizing radiation direct detection started in the 1950s with the first investigation of the conductivity induced by X- and γ-rays in insulating polymers as polyethylene, polymethyl methacrylate and polystyrene [6]. Nowadays the interest for the exploitation of organic materials as X-ray detectors is still very relevant thanks to their promising properties for such kind of applications. As they are based on Carbon and light weight atoms, their effective atomic number is similar to the average human tissue Z (7.64 for muscles) [7] and much lower than that of inorganic detectors based on heavier materials as Si, CdTe, CZT. Therefore, due to their low radiation stopping power, they could be exploited for medical dosimetric applications, since they might be interposed between the X-ray source and the patient providing a direct reliable real-time in situ dosimetry, without significantly absorbing the impinging beam. Indeed, the need to overcome the non-tissue equivalence of inorganic based detectors pushed the commercial spreading of X-ray diamond-based dosimeters [8], which however still have high manufacturing costs in covering large areas, similarly to other high performing detectors based on inorganic highly pure single crystals. Organic materials, on the other hand, are easily processable in liquid phase and thus they can be deposited over large areas by means of low-cost deposition techniques, e.g. inkjet printing [9][10][11]. Also, the possibility to deposit and to process them at low temperature, permits the fabrication of devices onto very thin and flexible plastic substrates, easily conformable to any kind of surface geometry [12][13]. Only few examples of direct ionizing radiation detectors based on organic semiconducting polymeric thin films are present in the literature [14][15], and some papers reported about the effects of high X-ray irradiation doses on organic materials [16][17]. However, because of the low atomic number of their constituent atoms, the interaction volume is small and the reported thin film (a few hundreds of nm thick) devices exhibited a limited detection sensitivity, due to their overall low attenuation efficiency. In order to overcome this limitation high-Z nanoparticles (metallic tantalum [18] and insulating bismuth oxide [15][11]) have been added to the semiconducting polymer enhancing the stopping power of the material. Another reported approach consists in improving the transport properties of the organic film by introducing high-mobility small molecules in a blend with the polymer, leading to enhanced performances of the detector [19]. The approach we proposed is to employ OSSCs as the active detection material in direct solid-state X-ray detectors, as it allows to easily override the above reported problems from several points of view. First of all, the possibility to grow large and thick (up to few mm^3) single crystals permits to enhance the attenuation efficiency of the device without the necessity to add high-Z elements to the organic material, thus preserving the tissue-equivalent feature of organic detectors. Moreover, the OSSCs high chemical purity, long-range order and lack of grain boundaries, typical of polymeric film-based devices, lead to unique transport properties, i.e. high carrier mobility [20], transport anisotropy [21][22] and long exciton diffusion lengths (up to 8 μm [23], very high if compared to that of 10 nm reported for organic thin film photovoltaic devices [24]). Also, some solution-grown organic crystals proved to be very robust to physical manipulation, to environmental conditions (air, light, room temperature) and to X-ray damage [1][2].

In this paper we report on X-ray solid state detectors based on Rubrene, considered as one of the highest performing single crystal for electronic applications, e.g. as active layer in Organic Field Effect Transistors (OFETs) [25], thanks to its very high carrier mobility (up to 20 cm^2/Vs [13]). We have fully characterized its performances as X-ray radiation detector under a Mo-target X-ray tube. Despite the several studies carried out on this molecular crystal, its application as active material in ionizing radiation detectors has not yet been investigated. Its detection features are compared to those of a recently reported OSSC-based X-ray direct detector, based on DNN (1,5-dinitronaphthalene), exhibiting a stable and reproducible response to X-rays at low bias voltages, in air and at room temperature [2]. In fact, since DNN crystals have much lower charge carrier mobility with respect to Rubrene, we intentionally compare the performances as X-ray detectors of these two types of crystals to investigate how the electrical performances of OSSCs, and in particular mobility, affect the radiation detection efficiency of OSSCs-based devices.

In more detail, we studied the X-ray photo-response of two series of Rubrene single crystals, which possess quite different electronic transport properties. These two sets of samples have been selected by directly measuring their charge carrier

Manuscript submitted on March 6, 2015. This work was supported in part from the European Community under the FP7-ICT Project "i-FLEXIS" (GA n. 611070).

L. Basiricò, A. Ciavatti and B. Fraboni are with the Department of Physics and Astronomy, University of Bologna, Bologna 40127, Italy (e-mail: laura.basirico2@unibo.it,andrea.ciavatti2@unibo.it, beatrice.fraboni@unibo.it).

M. Sibilia and A. Fraleoni-Morgera are with the Department of Engineering and Architecture, University of Trieste, Trieste 34100, Italy. A. Fraleoni-Morgera is also with Elettra Sincrotrone Trieste S.C.p.A, Basovizza (TS), Italy, and with CNR-NANO S3, Modena, Italy (e-mail: mirta.sibilia@phd.units.it, afraleoni@units.it).

S. Trabattoni and A. Sassella are with the Department of Materials Science, University of Milano Bicocca, Milan 20125, Italy (e-mail: silvia.trabattoni@mater.unimib.it, adele.sassella@mater.unimib.it, mailto:adele.sassella@ unimib.it).

mobility and dark current, i.e. the current flowing in the device in absence of radiation.
From this investigation we found out, very interestingly, that Rubrene-based detectors exhibited lower sensitivity to X-rays, poorer stability and reproducibility of the signal and a slower dynamic response in comparison to DNN-based devices, suggesting that the superior transport properties of Rubrene, in particular its much higher carrier mobility, are not key parameters for ionizing radiation detection in OSSCs.

II. Experimental

A. Crystal growth

DNN was purchased from Sigma Aldrich (97% purity). The compound was re-crystallized in chloroform until the compound melting point was stabilized in the range 214-215°C. The so-obtained crystals were hence used to prepare a saturated solution in acetone. Volumes of 5 mL from this solution were put into glass beakers, which were sealed with Al foil and parafilm. A small hole (approximatively 0.2 mm of diameter) was made in the center of the Al foil to allow slow and controlled solvent evaporation, and the growth batches were placed in a thermostatic room at 4°C. An optical microcopy image of one of the crystals obtained after complete solvent evaporation is reported in Fig. 1a. Rubrene powder was purchased from Acros Organics; single crystals (Fig. 1b) were grown by physical vapor transport (PVT) in a horizontal tube 75 cm long placed in a three-zone furnace with a temperature gradient of 2 °C/cm and a nitrogen flux of 50 mL/min, following the same method used in [22][26]. The chemical structures of Rubrene and DNN molecules are shown in Fig. 1c. The energy bandgap of the two materials is of 3.26 eV for DNN and 2.20 eV for Rubrene single crystals, in accordance with literature [27][28] and verified by means of optical absorption measurements.

B. Electrical characterization

Both Rubrene and DNN-based devices have been tested in a coplanar electrode configuration, as depicted in Fig. 1d. The electrodes have been deposited by thermal evaporation in high vacuum (10^{-6} torr) on the top of the crystals, along their axis of major growth, at a distance of about 45 µm, employing a shadow mask. In this way the highest π-orbital overlap direction, i.e. the crystal highest mobility axis, was electrically addressed for both crystals, in order to obtain comparable data for the samples tested. In such configuration the electric field is not uniform within the whole electrodes and over the entire semiconductor volume. In particular, the electric field is confined in a region of the crystal below the electrodes. The electric field distribution in a similar structure has been described by Chen et al. [29] for inorganic X-ray detectors based on amorphous selenium.
The crystal structures of Rubrene and DNN are reported in the literature [30][31][32]. All the electrical measurements were carried out in air, in dark and at room temperature, by means of a Keithley model 6517A electrometer.

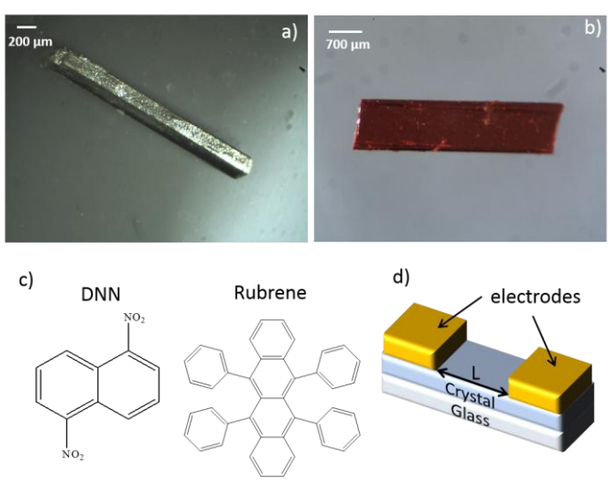

Fig. 1. Optical microscopy image of a DNN a) and Rubrene b) organic single crystal. c) Chemical structure of the DNN and Rubrene molecules, where H atoms are omitted. d) Schematic representation of the electrode configuration on single crystal based devices.

C. X-ray Irradiation

The X-ray irradiation measurements have been performed with a commercial X-ray tube with a Molybdenum target at 35 kV of accelerating voltage and for various filament currents, in order to scan different dose rates for detector sensitivity measurements: filament current in the range of 5-30 mA provides dose rates between 20 mGy/s and 120 mGy/s at 21 cm far from the source. The samples were placed in a metal box with a window of 4 cm^2, in such way the X-rays impinge on the sample without further filtration. At this position, the X-ray incident beam has a circular spot with a 5 mm diameter, covering entirely the detector surface. The electrodes and substrate contribution to X-ray induced signal is not negligible and will be discussed in more detail in Section III.

III. Results

A. Dark Current and Mobility

Fig. 2 reports the typical Current vs. Voltage curves of a) Rubrene and b) DNN based devices. Both curves follow the Space Charge Limited Current (SCLC) behavior, typical of high resistivity materials, as reported for other OSSCs [33]. Rubrene crystals have dark current (I_{OFF}) several orders of magnitude higher than those recorded for DNN, in the operating voltage range 5-100 V.

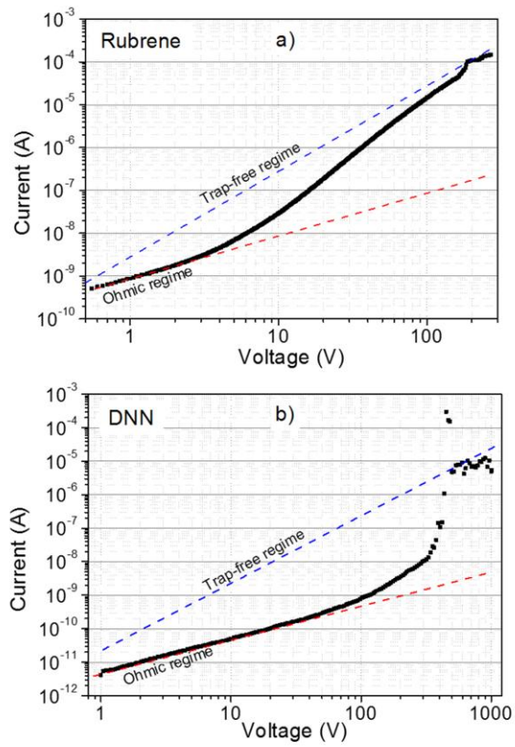

Fig. 2. Current vs. Voltage curve, for a) Rubrene (Rub1 set) and b) DNN based devices, in double-logarithmic scale within the space charge conduction regime. Note that the scales in the two graphs differ of about one order of magnitude.

We characterized two different sets of Rubrene crystals, one, named Rub1, with better electrical transport performances, i.e. with higher dark current and mobility up to 10 cm^2/Vs, indicating a higher crystal quality, and a less performing crystals set (Rub2), with average mobility values of 1.0 ± 0.5 cm^2/Vs.
The charge mobility of the molecular crystals has been estimated following the SCLC analyses method, reported for coplanar electrodes configuration [22]. The obtained values for the DNN and for the two sets of Rubrene crystals, averaged within five devices for each set, are reported in Table I.

TABLE I
Mobility, Dark Current, Sensitivity and Signal Amplitude values measured for DNN and Rubrene based detectors

Crystal	μ_{SCLC} cm^2/Vs	I_{OFF} @ 5V nA	S @ 5V nC/Gy	ΔI @ 5V nA
DNN	$(2.2 \pm 0.8)\times10^{-3}$	0.10 ± 0.05	3.3 ± 0.5	0.50 ± 0.10
Rub1	8 ± 2	4 ± 3	n.a.	n.a.
Rub2	1.0 ± 0.5	0.08 ± 0.05	1.4 ± 0.4	0.15 ± 0.10

Note that, even if the average charge mobility of some of the investigated Rubrene single crystals results one order of magnitude below the top-performing crystal reported in literature (charge mobility up to 20 cm^2/Vs has been reported for Rubrene based Organic Field Effect Transistors OFETs [20]), it remains at least two orders of magnitude higher than the average mobility recorded for DNN (see Table I).

B. *X-ray performances*

The dynamic behavior of the OSSC-based detectors was evaluated through the real-time recording of the current flowing within the crystal (Current vs. Time), at a fixed bias voltage, while switching ON and OFF the X-ray beam at regular time intervals. In this way, it is possible to assess not only the direct response of the detector, but also the dark current and the signal amplitude stability during the measurement. Fig. 3a shows the response of two different Rubrene crystals (one of set Rub1 and one of set Rub2), both biased at 5 V, exposed to 3 cycles of ON/OFF X-ray switching at a 120 mGy/s dose rate. Interestingly, we found that Rub1 samples, with higher mobility, exhibited a huge drift of the current baseline even at low biases (black line in Fig. 3a) and their signal response was not easily detectable. On the other hand, it was possible to detect a response signal from the lower mobility Rub2 samples, even if much weaker than the one typically obtained from DNN samples (Fig. 3b). Although a slight drift of the dark current is present also for Rub2 samples, a complete characterization as X-ray detectors could be carried out on them. On the other hand, the pronounced current instability of Rub1 samples, possibly ascribed to the higher dark current with respect to the other tested set of samples, makes them impracticable to characterize as detector, even though Rub 1 dark current average value is of the order of few nA, therefore still acceptable for a solid state radiation detector. Moreover DNN, which shows higher detection performances, has an average dark current value only one order of magnitude lower (≈0.1 nA) than Rub1 samples for identical bias voltage (5 V).

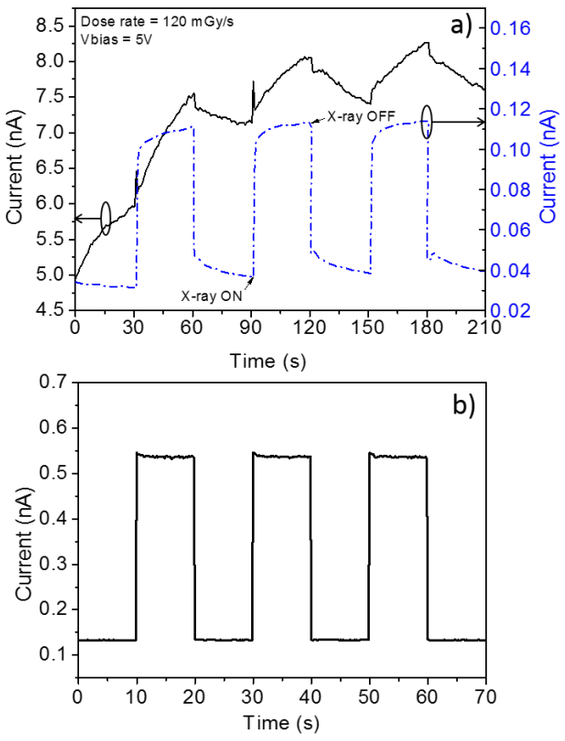

Fig. 3. Dynamical electrical response to X-rays, switched ON and OFF, of Rubrene single crystal devices: a) Rub1 (high dark current and mobility, black solid line - left y axis) and Rub2 (lower mobility, blue dashed line - right y axis); b) DNN. All samples were biased at 5V during the measurement and irradiated with a 120 mGy/s dose rate.

The Current vs. Voltage curves in a Rub2 sample for different X-ray dose rates are reported in Fig.4a. The instability of the dark current can be noticed by comparing the "Off" curves recorded with the X-ray beam off after each different dose rate exposure (the current shows a progressive decrease), possibly due to traps induced in Rubrene by X-ray exposure, as observed in literature [20]. The instability and lack of reproducibility of Rubrene electrical performances could be also ascribed to the huge sensitivity of this molecular crystal to environment conditions, as the detrimental effects of photo-oxidation on the transport properties of the crystal are reported in literature [34], even if still controversial [35]. Nonetheless, it is also well-known how single crystals are particularly stable to oxidation with respect to polycrystalline samples.

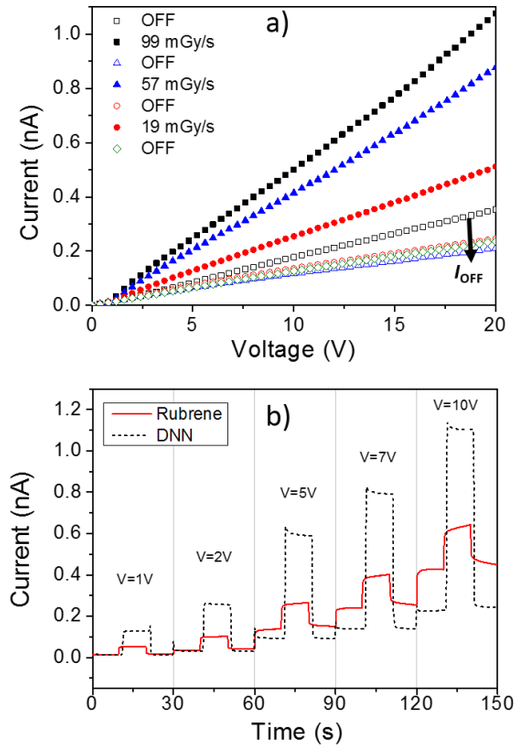

Fig. 4. a) Current vs. Voltage curves of Rub2-based detector in the dark (empty symbols) and under X-rays (filled symbols) at different dose rates. The dark current was recorded after each measurement under irradiation. The lack of overlapping between the dark current curves indicates the poor stability of the I_{OFF}. b) Current vs. Time curve the DNN-based (dashed black line) and Rubrene-based (continuous red line) device recorded while switching ON/OFF the X-ray beam (dose rate of 120 mGy/s) and sweeping the bias voltage after each cycle. The black arrow in a) indicates the progressive decrease of the dark current.

The X-ray induced photocurrent increases as the voltage increases, analogously to what has been reported for other studied OSSCs [1][2]; however, in the case of Rub2 crystals the baseline drift becomes pronounced at higher voltages (see Fig. 4b). Nevertheless, the X-ray induced photocurrent signal $\Delta I = I_{ON} - I_{OFF}$ was measured, considering as I_{OFF} the value just before the switching X-ray ON, for various radiation dose rates, sweeping the bias voltage up to 10 V and keeping the OFF and the ON state for 10 s each (Fig. 4b). From such measurements, we obtained the plot of the ΔI in function of the X-ray dose rate (Fig. 5). The detector sensitivity, defined as $S = \Delta I / D$, where D is the dose rate, could be thus extracted as the slope of the linear fit of the plot, and resulted to be about 1.4 nC/Gy at 5 V, more than 50% less than the one calculated for DNN-based devices biased at the same voltage with the same electrical configuration, as shown in Table I. Table I reports also the dark current I_{OFF} and the photocurrent response ΔI at a bias voltage of 5 V, together with the charge mobility values measured for the studied crystals. The errors were calculated considering the variability among five devices for each set. Fig. 5 reports the ΔI vs. D plots of the two devices, at the same bias voltage of 5 V: the signal response amplitude of Rub2-based detectors is much lower than that of DNN (about 0.2 nA for Rub2 vs. 0.5 nA for DNN at 5 V and 120 mGy/s dose rate) and their difference in sensitivity can be clearly observed comparing the much larger slope of the DNN plot with respect to that of Rub2. Fig. 5 also shows the current contribution recorded when the metal electrodes and the substrate are exposed to identical X-ray irradiation (i.e. without OSSC). This non-negligible X-ray induced photocurrent cannot be obviously ascribed to the organic crystal, it is rather a "background signal" that has to be subtracted from the total collected signal in order to obtain the intrinsic crystal response to the radiation of OSSCs-based detectors. As shown in Fig. 5, the X-ray photo-response of

Rubrene detectors is quite low, barely distinguishable from the background (electrodes and substrate) contribution.

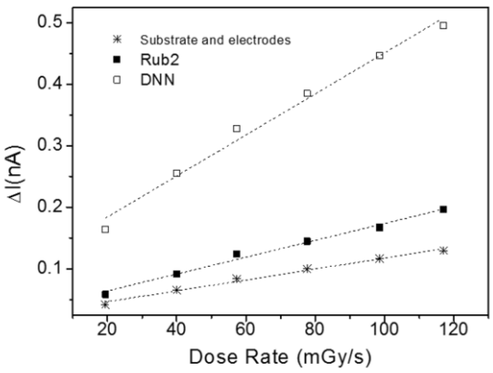

Fig. 5. Rub2 (full squares) and DNN (empty squares) X-ray induced current signal $\Delta I = I_{ON} - I_{OFF}$ for increasing dose rates biased at 5 V. From the slope of the linear fit of the plots, the sensitivity can be estimated for the two detectors. The electrodes/substrate X-ray induced photocurrent, i.e. the "background signal" measured in the absence of the OSSC, is also reported (black stars).

The above reported poorer performances of Rubrene-based X-ray detectors compared to DNN ones suggest that in X-ray detectors based on organic single crystals a high mobility value does not assure an improvement of the X-ray detection sensitivity and, in general, of the detector performances. Such a behavior is in good agreement with the results reported on 4-hydroxycyanobenzene (4HCB) crystals when tested as X-ray detectors [1][2]. In fact, 4HCB crystals are characterized by anisotropic transport properties, poorer than Rubrene (max. mobility <0.01 cm^2/Vs)[21], but show a very strong and stable X-ray photo-response which is maximum along the crystal axis with lower mobility values (min. mobility $<1\times10^{-5}$ cm^2/Vs)[2][21].

On the contrary, a direct positive correlation between the X-ray irradiation sensitivity and the charge carrier mobility was found for organic X-ray detectors based on polymeric thin films [19]. Such a different behavior for polymeric thin films and the here reported OSSCs, in line with the mentioned evidences recorded for 4HCB, could be understood and justified by two considerations:

1) the mobility of the polymeric films varies in the range 1.3×10^{-6} - 2.2×10^{-5} cm^2/Vs, i.e. between very small values in comparison to those measured for our devices, which are at least two orders of magnitude higher and therefore already assure an efficient electronic transport within the device;

2) organic single crystals are characterized by the absence of grain boundaries and thus by a much lower density of traps, which is reflected in a much higher carrier lifetime τ than in organic thin films.

In other words, the above reported results strongly suggest that in the case of OSSCs-based detectors the intrinsic μτ product, a fundamental parameter that controls the charge collection efficiency of radiation detectors, could be more sensitive to τ than to μ when the carrier mobility is large enough to grant efficient charge collection, as in the case of OSSCs.

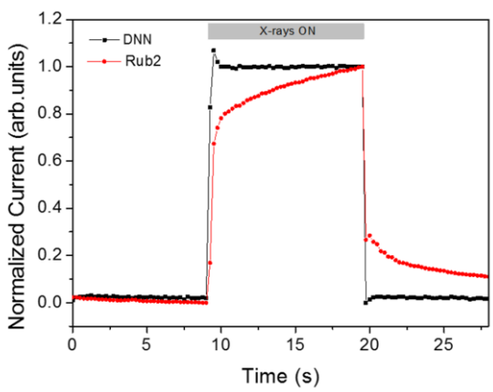

Fig. 6. Rub2 (red circles) and DNN (black squares) normalized current response upon switching ON and OFF the X-ray beam. The samples are both biased at 50V. The rise and fall times of the signal of Rubrene-based devices are both much longer than that of DNN-based detectors.

In addition, very interestingly, a quite different dynamic behavior of the X-ray induced photocurrent signal can be observed by directly comparing the normalized Current vs. Time curves of a DNN and a Rub2 detectors while switching ON and OFF the X-ray beam (Fig. 6). Rubrene-based devices exhibit current rise and decay times longer than the DNN ones. Both the rise and decay time of well performing DNN devices are less than 100 ms, which is the sampling rate of the instrument, while for Rubrene-based devices both exceed tens of seconds. Slow decay times were also observed in preliminary pioneering studies on the X-ray induced conductivity in organic insulating materials (e.g. amber, polyethylene, polystyrene) and were related to the presence and distribution of trapping sites in the material [6]. Moreover, Mathews et al. [36] observed a slow current decay for an Organic Field Effect Transistor (OFET) based on Rubrene single crystal after continuous illumination with a 405 nm blue laser. They argued that the electron traps induced by oxidation in Rubrene lower the electron/hole recombination rate. In particular, photo-generated excitons dissociate in these oxygen-related trap sites, as a consequence the electrons remain trapped while holes drift toward the channel. As a result the electron/hole recombination rate decreases and gives rise to slow current decay. An analogous mechanism may occur in the here studied Rubrene-based detectors after turning OFF X-rays. These observations hint at a correlation between the slow response of Rubrene-based detectors and the trap states present also in high purity, PVT grown Rubrene single crystals, possibly induced by the exposure to oxygen and visible light [37][34]. We demonstrated, on the other hand, that DNN and 4HCB solution grown crystals are stable in air and show a very low sensitivity to environment exposure [2]. Further measurements are ongoing in order to better understand the role of traps in organic crystals when used as X-ray detectors and to gain a better insight on the correlation between the charge collection mechanisms, the carrier mobility and the crystal molecular structure in organic single crystals-based ionizing radiation detectors.

IV. Conclusions

To summarize, we demonstrated how organic single crystals offer a great potential as novel low cost materials in the field of solid-state radiation detection. In particular this study represents the first investigation on direct solid-state X-ray detectors based on Rubrene, the most studied among organic single crystals. We compared the X-ray detection performances of Rubrene, characterized by a high conductivity and mobility, with those of DNN-based devices, having two orders of magnitude lower mobility and representing one of the few examples of OSSC-based detector reported in literature. Rubrene-based detectors exhibit halved sensitivity values, poorer output signal amplitude and stability with respect to DNN-based ones. The dark current of Rubrene detectors is unstable and decreases after X-ray exposure. Moreover, a much slower response to X-rays (rise and decay times over 10 s) has been observed for Rubrene detectors. Since the average mobility of the investigated Rubrene samples is 1.0 ± 0.5 cm^2/Vs, two orders of magnitude higher than DNN ((2.2 ± 0.8)×10^{-3} cm^2/Vs), our results clearly indicate that a high charge mobility does not represent a key parameter to achieve high detecting performances in organic single crystal-based ionizing radiation detectors. Possibly, the sensitivity of Rubrene to environmental conditions could affect the reproducibility, the stability and the dynamic of the X-ray induced photocurrent signal. The here reported findings give an insight into the understanding of the key parameters and physical properties to take into account for the development of a novel class of solid state X-ray detectors based on OSSCs.

References

[1] B. Fraboni, A. Ciavatti, F. Merlo, L. Pasquini, A. Cavallini, A. Quaranta, A. Bonfiglio, and A. Fraleoni-Morgera, "Organic Semiconducting Single Crystals as Next Generation of Low-Cost, Room-Temperature Electrical X-ray Detectors," *Adv. Mater.*, vol. 24, no. 17, pp. 2289–2293, May 2012.

[2] B. Fraboni, A. Ciavatti, L. Basiricò, and A. Fraleoni-Morgera, "Organic semiconducting single crystals as solid-state sensors for ionizing radiation," *Faraday Discuss.*, vol. 174, no. 0, pp. 219–234, Dec. 2014.

[3] G. Hull, N. P. Zaitseva, N. J. Cherepy, J. R. Newby, W. Stoeffl, and S. A. Payne, "New Organic Crystals for Pulse Shape Discrimination," *IEEE Trans. Nucl. Sci.*, vol. 56, no. 3, pp. 899–903, Jun. 2009.

[4] T. Agostinelli, M. Campoy-Quiles, J. C. Blakesley, R. Speller, D. D. C. Bradley, and J. Nelson, "A polymer/fullerene based photodetector with extremely low dark current for x-ray medical imaging applications," *Appl. Phys. Lett.*, vol. 93, no. 20, pp. 203305–203305–3, Nov. 2008.

[5] P. E. Keivanidis, N. C. Greenham, H. Sirringhaus, R. H. Friend, J. C. Blakesley, R. Speller, M. Campoy-Quiles, T. Agostinelli, D. D. C. Bradley, and J. Nelson, "X-ray stability and response of polymeric photodiodes for imaging applications," *Appl. Phys. Lett.*, vol. 92, no. 2, pp. 023304–023304–3, Jan. 2008.

[6] J. F. Fowler, "X-Ray Induced Conductivity in Insulating Materials," *Proc. R. Soc. Lond. Math. Phys. Eng. Sci.*, vol. 236, no. 1207, pp. 464–480, Sep. 1956.

[7] M. Bruzzi, M. Bucciolini, F. Nava, S. Pini, and S. Russo, "Advanced materials in radiation dosimetry," *Nucl. Instrum. Methods Phys. Res. Sect. Accel. Spectrometers Detect. Assoc. Equip.*, vol. 485, no. 1–2, pp. 172–177, Jun. 2002.

[8] M. Bruzzi, M. Bucciolini, G. A. P. Cirrone, G. Cuttone, A. Guasti, S. Mazzocchi, S. Pirollo, M. G. Sabini, and S. Sciortino, "Characterization of CVD diamond films as radiation detectors for dosimetric applications," *IEEE Trans. Nucl. Sci.*, vol. 47, no. 4, pp. 1430–1433, Aug. 2000.

[9] A. Teichler, J. Perelaer, and U. S. Schubert, "Inkjet printing of organic electronics – comparison of deposition techniques and state-of-the-art developments," *J. Mater. Chem. C*, vol. 1, no. 10, pp. 1910–1925, Feb. 2013.

[10] L. Basiricò, P. Cosseddu, B. Fraboni, and A. Bonfiglio, "Inkjet printing of transparent, flexible, organic transistors," *Thin Solid Films*, vol. 520, no. 4, pp. 1291–1294, Dec. 2011.

[11] H. Sirringhaus, T. Kawase, R. H. Friend, T. Shimoda, M. Inbasekaran, W. Wu, and E. P. Woo, "High-Resolution Inkjet Printing of All-Polymer Transistor Circuits," *Science*, vol. 290, no. 5499, pp. 2123–2126, Dec. 2000.

[12] A. L. Briseno, S. C. B. Mannsfeld, M. M. Ling, S. Liu, R. J. Tseng, C. Reese, M. E. Roberts, Y. Yang, F. Wudl, and Z. Bao, "Patterning organic single-crystal transistor arrays," *Nature*, vol. 444, no. 7121, pp. 913–917, Dec. 2006.

[13] T. Someya, T. Sekitani, S. Iba, Y. Kato, H. Kawaguchi, and T. Sakurai, "A large-area, flexible pressure sensor matrix with organic field-effect transistors for artificial skin applications," *Proc. Natl. Acad. Sci. U. S. A.*, vol. 101, no. 27, pp. 9966–9970, Jul. 2004.

[14] F. A. Boroumand, M. Zhu, A. B. Dalton, J. L. Keddie, P. J. Sellin, and J. J. Gutierrez, "Direct x-ray detection with conjugated polymer devices," *Appl. Phys. Lett.*, vol. 91, no. 3, p. 033509, Jul. 2007.

[15] A. Intaniwet, C. A. Mills, M. Shkunov, P. J. Sellin, and J. L. Keddie, "Heavy metallic oxide nanoparticles for enhanced sensitivity in semiconducting polymer x-ray detectors," *Nanotechnology*, vol. 23, no. 23, p. 235502, Jun. 2012.

[16] C. R. Newman, H. Sirringhaus, J. C. Blakesley, and R. Speller, "Stability of polymeric thin film transistors for x-ray imaging applications," *Appl. Phys. Lett.*, vol. 91, no. 14, p. 142105, 2007.

[17] M.-M. L. R. A. B. Devine, "X-ray irradiation effects in top contact, pentacene based field effect transistors for space related applications," *Appl. Phys. Lett.*, vol. 88, no. 15, pp. 151907–151907–3, 2006.

[18] C. A. Mills, H. Al-Otaibi, A. Intaniwet, M. Shkunov, S. Pani, J. L. Keddie, and P. J. Sellin, "Enhanced x-ray detection sensitivity in semiconducting polymer diodes containing metallic nanoparticles," *J. Phys. Appl. Phys.*, vol. 46, no. 27, p. 275102, Jul. 2013.

[19] A. Intaniwet, J. L. Keddie, M. Shkunov, and P. J. Sellin, "High charge-carrier mobilities in blends of poly(triarylamine) and TIPS-pentacene leading to better performing X-ray sensors," *Org. Electron.*, vol. 12, no. 11, pp. 1903–1908, Nov. 2011.

[20] V. Podzorov, E. Menard, A. Borissov, V. Kiryukhin, J. A. Rogers, and M. E. Gershenson, "Intrinsic Charge Transport on the Surface of Organic Semiconductors," *Phys. Rev. Lett.*, vol. 93, no. 8, p. 086602, Aug. 2004.

[21] B. Fraboni, C. Femoni, I. Mencarelli, L. Setti, R. Di Pietro, A. Cavallini, and A. Fraleoni-Morgera, "Solution-Grown, Macroscopic Organic Single Crystals Exhibiting Three-Dimensional Anisotropic Charge-Transport Properties," *Adv. Mater.*, vol. 21, no. 18, pp. 1835–1839, 2009.

[22] D. Braga, N. Battaglini, A. Yassar, G. Horowitz, M. Campione, A.Sassella and A. Borghesi, "Bulk electrical properties of rubrene single crystals: Measurements and analysis," *Phys. Rev. B*, vol. 77, no. 11, p. 115205 1–7, 2008.

[23] H. Najafov, B. Lee, Q. Zhou, L. C. Feldman, and V. Podzorov, "Observation of long-range exciton diffusion in highly ordered organic semiconductors," *Nat. Mater.*, vol. 9, no. 11, pp. 938–943, Nov. 2010.

[24] K.-J. Baeg, M. Binda, D. Natali, M. Caironi, and Y.-Y. Noh, "Organic Light Detectors: Photodiodes and Phototransistors," *Adv. Mater.*, vol. 25, no. 31, pp. 4267–4295, Aug. 2013.

[25] D. Braga and G. Horowitz, "High-Performance Organic Field-Effect Transistors," *Adv. Mater.*, vol. 21, no. 14–15, pp. 1473–1486, Apr. 2009.

[26] R. A. Laudise, C. Kloc, P. G. Simpkins, and T. Siegrist, "Physical vapor growth of organic semiconductors," *J. Cryst. Growth*, vol. 187, no. 3–4, pp. 449–454, May 1998.

[27] M. Kojima, J. Tanaka, and S. Nagakura, "The electronic spectrum and electronic structure of 1,5 dinitronaphthialene," *Theor. Chim. Acta*, vol. 3, no. 5, pp. 432–438, Jan. 1965.

[28] S. Tavazzi, A. Borghesi, A. Papagni, P. Spearman, L. Silvestri, A. Yassar, A. Camposeo, M. Polo, and D. Pisignano, "Optical response and emission waveguiding in rubrene crystals," *Phys. Rev. B*, vol. 75, no. 24, p. 245416, Jun. 2007.

[29] F. Chen, K. Wang, Y. Fang, N. Allec, G. Belev, S. O. Kasap, and K. S. Karim, "Direct-Conversion X-Ray Detector Using Lateral Amorphous Selenium Structure," *IEEE Sens. J.*, vol. 11, no. 2, pp. 505–509, Feb. 2011.

[30] O. D. Jurchescu, A. Meetsma, and T. T. M. Palstra, "Low-temperature structure of rubrene single crystals grown by vapor transport," *Acta Crystallogr. B*, vol. 62, no. 2, pp. 330–334, Apr. 2006.

[31] B. D. Chapman, A. Checco, R. Pindak, T. Siegrist, and C. Kloc, "Dislocations and grain boundaries in semiconducting rubrene single-crystals," *J. Cryst. Growth*, vol. 290, no. 2, pp. 479–484, May 2006.

[32] J. Trotter, "The crystal structure of 1,5-dinitronaphthalene," *Acta Crystallogr.*, vol. 13, no. 2, pp. 95–99, 1960.

[33] R. W. I. de Boer, M. Jochemsen, T. M. Klapwijk, A. F. Morpurgo, J. Niemax, A. K. Tripathi, and J. Pflaum, "Space Charge Limited Transport and Time of Flight Measurements in Tetracene Single Crystals: a Comparative Study," *J. Appl. Phys.*, vol. 95, no. 3, p. 1196, 2004.

[34] H. Najafov, D. Mastrogiovanni, E. Garfunkel, L. C. Feldman, and V. Podzorov, "Photon-Assisted Oxygen Diffusion and Oxygen-Related Traps in Organic Semiconductors," *Adv. Mater.*, vol. 23, no. 8, pp. 981–985, 2011.

[35] O. Mitrofanov, D. V. Lang, C. Kloc, J. M. Wikberg, T. Siegrist, W.-Y. So, M. A. Sergent, and A. P. Ramirez, "Oxygen-Related Band Gap State in Single Crystal Rubrene," *Phys. Rev. Lett.*, vol. 97, no. 16, p. 166601, Oct. 2006.

[36] N. Mathews, D. Fichou, E. Menard, V. Podzorov, and S. G. Mhaisalkar, "Steady-state and transient photocurrents

in rubrene single crystal free-space dielectric transistors," *Appl. Phys. Lett.*, vol. 91, no. 21, p. 212108, Nov. 2007.

[37] C. Krellner, S. Haas, C. Goldmann, K. P. Pernstich, D. J. Gundlach, and B. Batlogg, "Density of bulk trap states in organic semiconductor crystals: Discrete levels induced by oxygen in rubrene," *Phys. Rev. B*, vol. 75, no. 24, p. 245115, Jun. 2007.

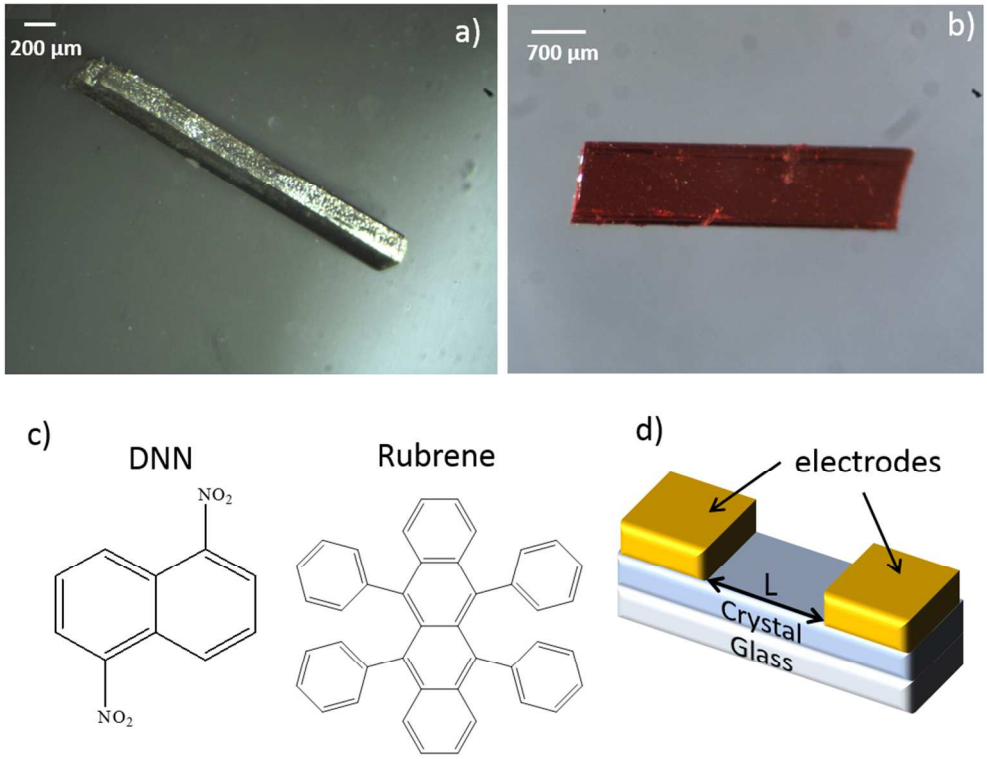

Optical microscopy image of a DNN a) and Rubrene b) organic single crystal. c) Chemical structure of the DNN and Rubrene molecules, where H atoms are omitted. d) Schematic representation of the electrode configuration on single crystal based devices.
92x70mm (300 x 300 DPI)

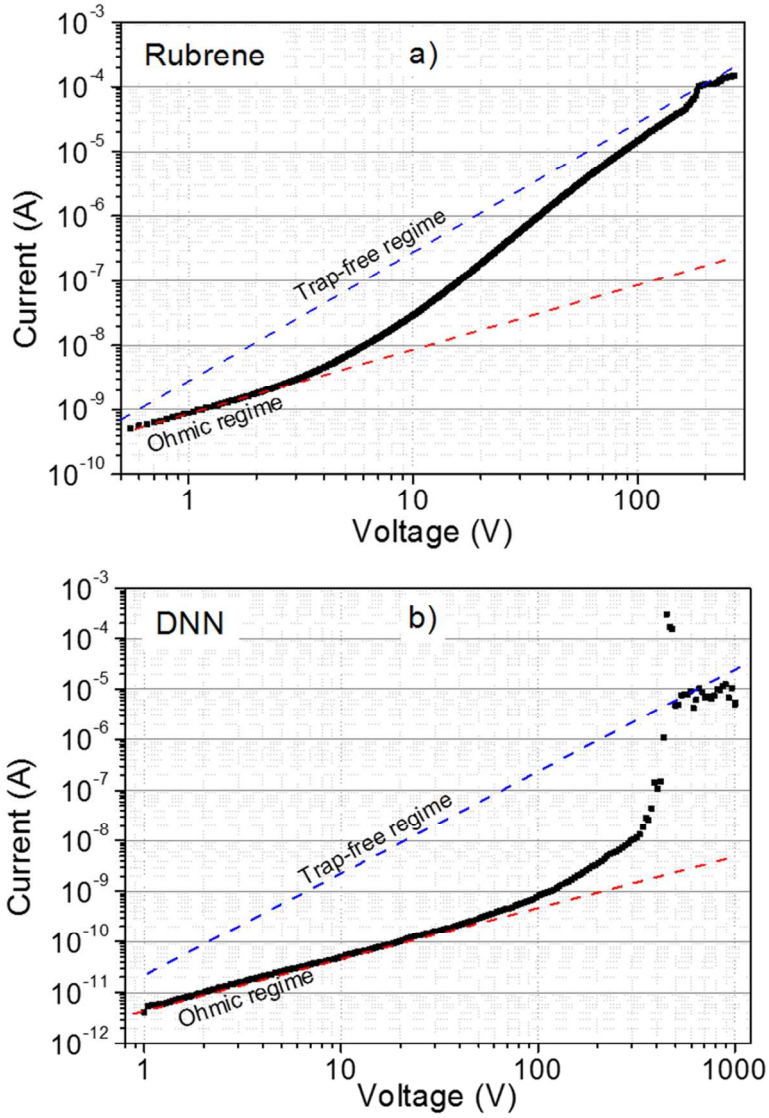

Current vs. Voltage curve, for a) Rubrene (Rub1 set) and b) DNN based devices, in double-logarithmic scale within the space charge conduction regime. Note that the scales in the two graphs differ of about one order of magnitude.
114x149mm (300 x 300 DPI)

Crystal	μ_{SCLC} cm^2/Vs	I_{OFF} @ 5V nA	S @ 5V nC/Gy	ΔI @ 5V nA
DNN	$(2.2 \pm 0.8) \times 10^{-3}$	0.10 ± 0.05	3.3 ± 0.5	0.50 ± 0.10
Rub1	8 ± 2	4 ± 3	n.a.	n.a.
Rub2	1.0 ± 0.5	0.08 ± 0.05	1.4 ± 0.4	0.15 ± 0.10

MOBILITY, DARK CURRENT, SENSITIVITY AND SIGNAL AMPLITUDE VALUES MEASURED FOR DNN AND RUBRENE BASED DETECTORS
21x5mm (600 x 600 DPI)

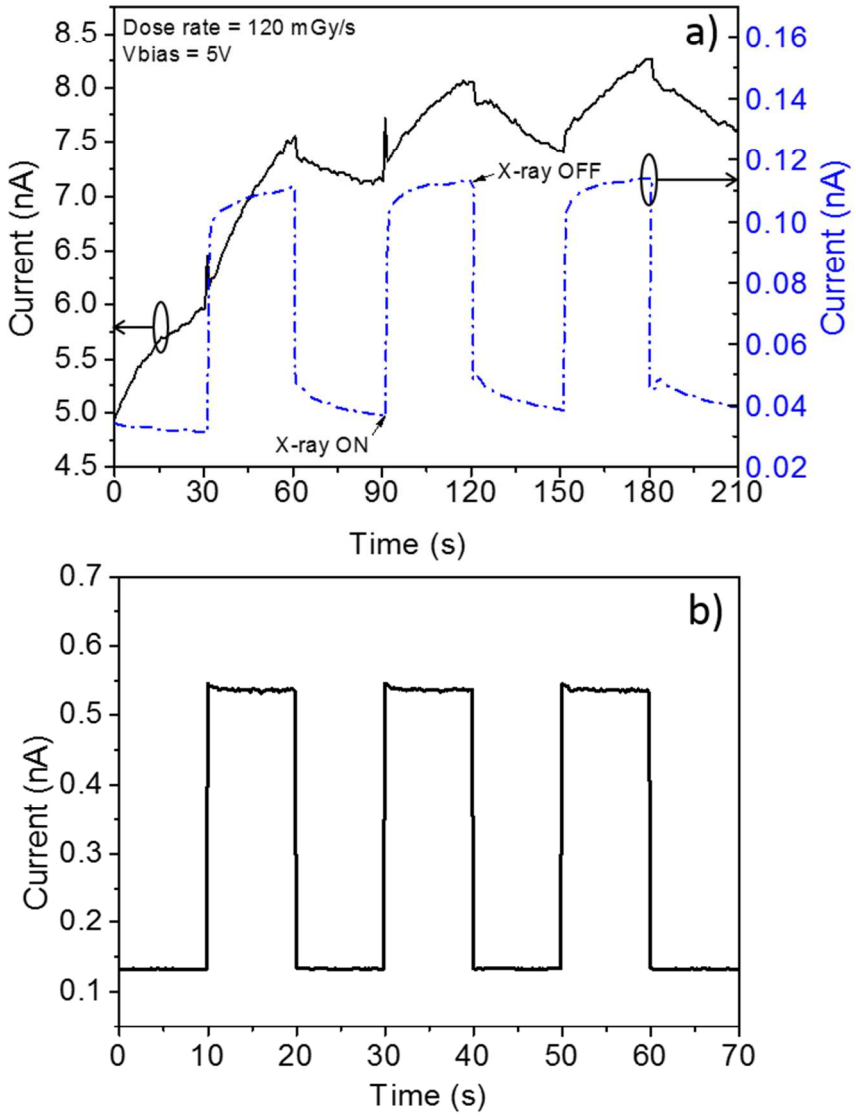

Dynamical electrical response to X-rays, switched ON and OFF, of Rubrene single crystal devices: a) Rub1 (high dark current and mobility, black solid line - left y axis) and Rub2 (lower mobility, blue dashed line - right y axis); b) DNN. All samples were biased at 5V during the measurement and irradiated with a 120 mGy/s dose rate.
64x85mm (300 x 300 DPI)

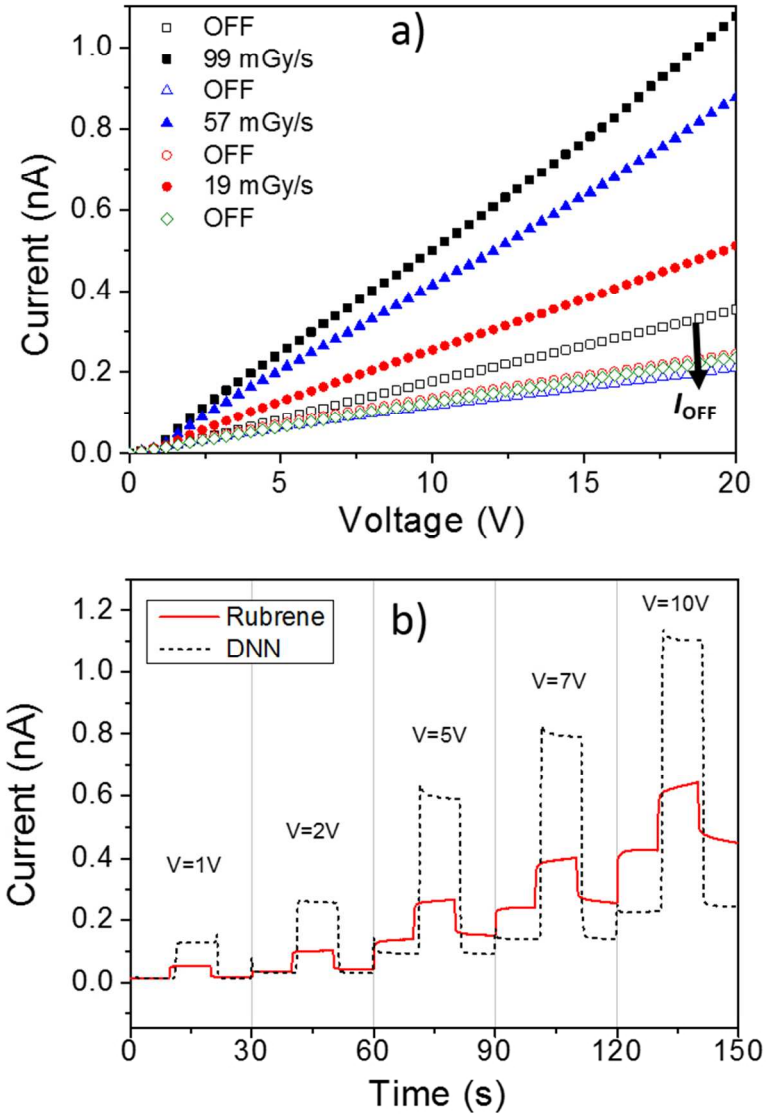

a) Current vs. Voltage curves of Rub2-based detector in the dark (empty symbols) and under X-rays (filled symbols) at different dose rates. The dark current was recorded after each measurement under irradiation. The lack of overlapping between the dark current curves indicates the poor stability of the IOFF. b) Current vs. Time curve the DNN-based (dashed black line) and Rubrene-based (continuous red line) device recorded while switching ON/OFF the X-ray beam (dose rate of 120 mGy/s) and sweeping the bias voltage after each cycle. The black arrow in a) indicates the progressive decrease of the dark current.
67x91mm (300 x 300 DPI)

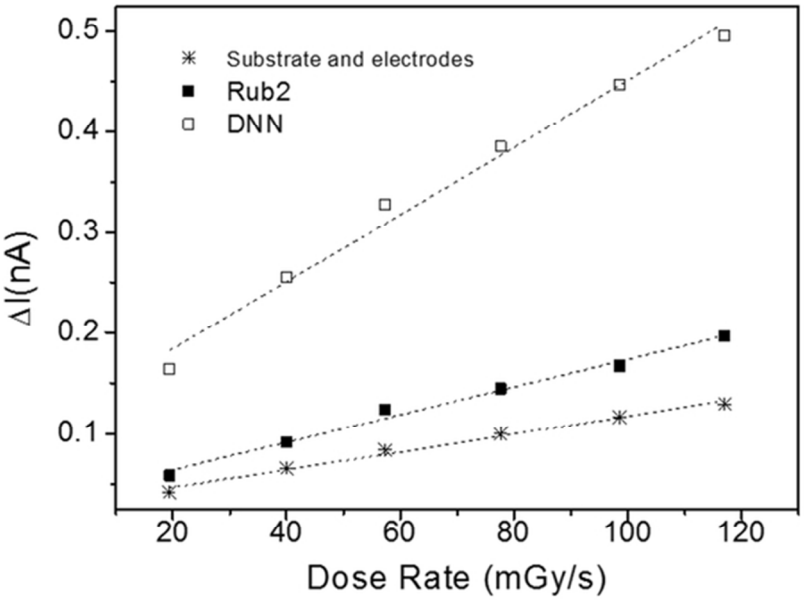

Rub2 (full squares) and DNN (empty squares) X-ray induced current signal ΔI=I_ON-I_OFF for increasing dose rates biased at 5 V. From the slope of the linear fit of the plots, the sensitivity can be estimated for the two detectors. The electrodes/substrate X-ray induced photocurrent, i.e. the "background signal" measured in the absence of the OSSC, is also reported (black stars).
61x43mm (300 x 300 DPI)

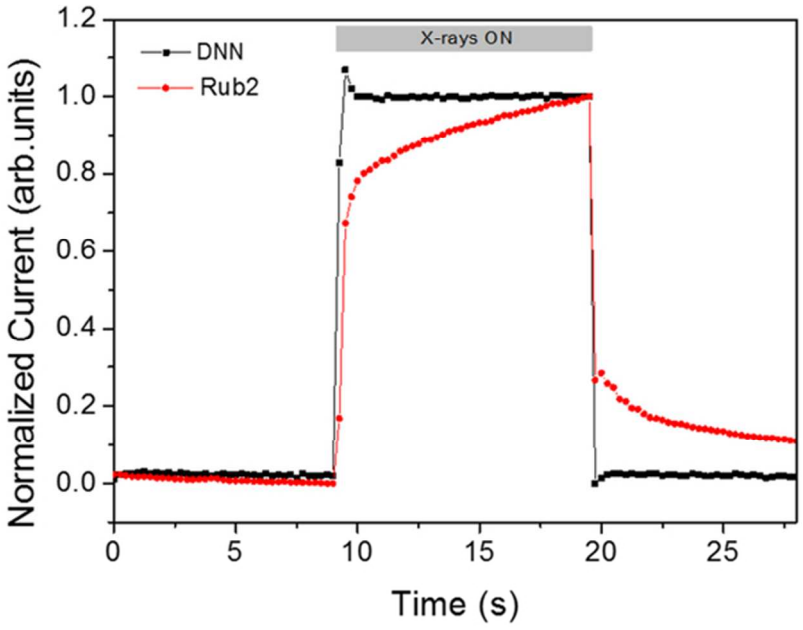

Rub2 (red circles) and DNN (black squares) normalized current response upon switching ON and OFF the X-ray beam. The samples are both biased at 50V. The rise and fall times of the signal of Rubrene-based devices are both much longer than that of DNN-based detectors.
61x43mm (300 x 300 DPI)